

A single-molecule study of inhibition effect of Naringenin on transforming growth factor- β ligand-receptor binding

Yong Yang^a, Yongchun Xu^a, Tie Xia^a, Fangjin Chen^c, Chunling Zhang^b, Wei Liang^b, Luhua Lai^c, Xiaohong Fang^{a*}

^a Beijing National Laboratory for Molecular Sciences, Institute of Chemistry, Key Laboratory of Molecular Nanostructures and Nanotechnology, Chinese Academy of Sciences, Beijing 100190, P.R. China, Tel & Fax: 86-10-62650024

^b Protein & Peptide Pharmaceutical Laboratory, National Laboratory of Biomacromolecules, Institute of Biophysics, Chinese Academy of Sciences, 15 Datun Road, Beijing 100101, P.R. China.

^c Beijing National Laboratory for Molecular Sciences, State Key Laboratory for Structural Chemistry of Unstable and Stable Species College of Chemistry and Molecular Engineering, Peking University, Beijing 100871, P.R. China.

SUPPLEMENTARY INFORMATION

Experimental Section

Cell Culture and Transfection. HeLa cells were cultured in DMEM (Gibco) supplemented with 10% FBS (HyClone) at 37°C in 5% CO₂. R1B cells were maintained in MEM containing 10% FBS. The DNA fragment encoding full-length

T β RII was subcloned into the HindIII and BamHI sites of pEGFP-N1 (Clontech), yielding the T β RII-GFP expression plasmid¹. Transfection of T β RII-GFP plasmid was performed using lipofectamine2000 (invitrogen). Cells growing in a 35-mm glass-bottom dish (Shengyou Biotechnology) were transfected with 0.2 μ g/mL plasmid in the phenol red-free DMEM. To achieve a low-level protein expression, cells were incubated with the plasmid for 4 h, washed, and then imaged in the phenol red-free DMEM under the fluorescence microscopy.

For Naringenin or SB431542 treatment, the transfected cells which were ready for single-molecule imaging were incubated with 50 μ M Naringenin, 100 μ M Naringenin or 100 μ M SB431542 (Shanxi Biotechnology) in the phenol red-free DMEM for 1h at 37°C before fluorescence imaging. For the ligand stimulation experiment, the transfected cells were incubated with 10 ng/mL TGF- β 1 (R&D) in the phenol red-free DMEM for 15 min at 37°C.

Single-Molecule Fluorescence Imaging. Single-molecule fluorescence imaging was performed with the objective-type total internal reflection fluorescence microscopy using an inverted microscope (IX 71, Olympus, Japan), a total internal reflective fluorescence illuminator, a 100X/1.45NA Plan Apochromat TIR objective (Olympus, Japan) and a 14-bit back-illuminated electron-multiplying charge-coupled device (EMCCD) (Andor iXon DU-897 BV).¹ The microscope was equipped with a CO₂ incubation system (INU-ZIL-F1, TOKAI HIT) and live cell imaging was performed at 37°C in 5% CO₂. GFP was excited at 488-nm by an argon laser (Melles Griot,

Carlsbad, CA) with the power of 5 mW measured after the laser passing through the objective in the epi-fluorescence mode. The collected fluorescent signals were passed through two filters, BA510IF and HQ 525/50 (Chroma Technology), before directed to the EMCCD. The gain of EMCCD was set at 300. Only the central quarter of the chip (256×256 pixels) was used for imaging analysis to ensure homogeneous illumination. Movies of 200 frames were acquired for each sample at a frame rate of 10 Hz using MetaMorph software (Molecular Device).

For the photobleaching-step counting study, before the single-molecule fluorescence imaging, the cells were washed with cold PBS (4°C) twice and fixed in cold 4% paraformaldehyde/PBS solution for 10 min.

For the control experiment of single GFP molecule imaged on coverslip, GFP protein purified from *E. coli* was firstly dissolved in the high salt buffer (600 mM NaCl, 150 mM PBS buffer, pH 7.4) to prevent the dimer formation and then immobilized on the coverslips through biotin coupled GFP antibody (Clontech) as previously reported¹.

Image Analysis. For analysis of single-molecule fluorescence intensity in a movie acquired from living cells, the background fluorescence was first subtracted from each frame using the rolling ball method in Image J software (National Institute of Health). Then the first frame of each movie was used for fluorescent spot (regions of interest) selection. The image was thresholded (four times of the mean intensity of an area with no fluorescent spots), then filtered again with a user-defined program in Matlab.¹

To analyze the photobleaching steps, regions of interest for bleaching analysis were selected according to the method previously reported¹. The background fluorescence was subtracted from the movie acquired from the fixed cells using the rolling ball method in Image J software.

AFM Force Measurement. Preparations of chemical modification of AFM tips (type: NP, from Veeco, Santa Barbara, CA, USA) and T β RII extracellular domain were carried out as we previous reported.² The force measurements of the TGF- β 1-modified AFM tip on the living HeLa and R1B cells were carried out on a PicoSPM II with PicoScan 3000 controller and a large scanner (Molecular Imaging, Tempe, AZ). The AFM scanner was mounted on an inverted fluorescence microscopy (Olympus IX71, Japan). The loading rate of force measurements was 1.0×10^4 pN/s. The force curves measured in living HeLa and R1B cells were recorded and analyzed by PicoScan 5 software (Molecular Imaging, Tempe, AZ). All forces were measured with contact mode at room temperature.

Theoretic study with molecular docking and molecular dynamics. Molecular docking study was carried out for the extracellular domain of T β RII and Naringenin using AutoDock 4.³ The T β RII coordinates were downloaded from the Protein Data Bank (PDB code 1PLO, first NMR structure).⁴ ArgusLab4.0.1⁵ and UFF force field were used to prepare the small molecule structure. The Lamarckian genetic algorithm implemented in AutoDock 4 was used for sampling. In general, the docking

parameters for AutoDock4³ were kept to default values. The following parameters were modified from default: number of GA runs was set to 45, number of individuals in the population was set to 300, maximum numbers of energy evaluations were set to 5×10^7 , and maximum number of generations was set to 2700. A $106\text{\AA} \times 100\text{\AA} \times 108\text{\AA}$ grid map was used in all docking calculations. The resulting conformations were clustered and the lowest energy conformation from the largest cluster was chosen for further molecular dynamics (MDs) simulation.⁶ The estimated binding free energy for this structure is -7.31kcal/mol.

MD simulations were carried out for two systems: the human T β RII extracellular domain (1PLO1, the first structure of the NMR structure) and its complex with Naringenin (1PLO1_INB) using AMBER10 with the parm99 AMBER force field.⁷ All the protonation states of histidine residues were treated as HID (ND1-protonated) form. The systems were neutralized and immersed in an octahedral periodic box of TIP3P⁸ water molecules with a closeness parameter of 8 \AA away from the boundary of any atoms.

The final system for the human T β RII extracellular domain-Naringenin complex (1PLO1_INB) contains 6213 waters and 7 Na^+ ions, with a volume of 240883.484\AA^3 (oct). And the human T β RII extracellular domain system contains 6224 waters and 7 Na^+ ions with a volume of 241131.398\AA^3 (oct).

The Ewald method⁹ was used for the treatment of long range electrostatic interactions and the SHAKE algorithm¹⁰ were used for constraining all bonds involving hydrogen atoms. The non-bond interaction cutoff was set to 8.0 \AA . Energy

minimization was performed for each solvated complex using the conjugate gradient algorithm, harmonic constraints were applied with a force constant gradually relaxed from 2 kcal/Å. After minimization, all systems were heated up from 0K to 310 K during 50 ps, then 50 ps density equilibration at 310 K with weak restraints on the complex (2kcal/Å). Production runs were carried out for more than 22ns at 310 K. An integration time-step of 2 fs was used and structures were saved every 4 ps. The systems were run with constant pressure and temperature (NPT ensemble mode) with periodic boundary conditions. Constant pressure was maintained using the Langevin piston method¹¹ with a 1 kDa pressure piston, a piston collision frequency of 2 ps⁻¹.

The root-mean-square deviation (RMSD) of the protein backbone non-hydrogen atoms (the 11 residues at the C terminal and 10 residues at the N terminal were not included) relative to the first structure through the MD simulations were calculated and plotted in Fig S4. After 12ns equilibration, the fluctuations of the two systems became almost constant. For the NMR structure of TβRII, the average RMSD after 12ns was $2.69\pm0.12\text{\AA}$. In contrast, the complex structure of TβRII binding with Naringenin became more flexible with an average RMSD of $4.95\pm0.17\text{\AA}$. We also carried out MD simulations for the TβRI, TβRII and TGF-β1 complex (crystal structure, PDB code 3KFD¹²), in which the TβRII molecule varied little and adopted highly similar structure compared to the first NMR structure from 1PLO1 (RMSD of 0.94 Å).

Therefore, our docking calculation showed that Naringenin can bind to TβRII and the following MD simulations indicated that the binding of Naringenin significantly

changed the T β RII conformation dynamics by increasing its flexibility. As a result, treating T β RII with Naringenin might reduce the binding probability of T β RII with TGF- β 1, which is in accordance with the single molecule study.

Supporting Figures

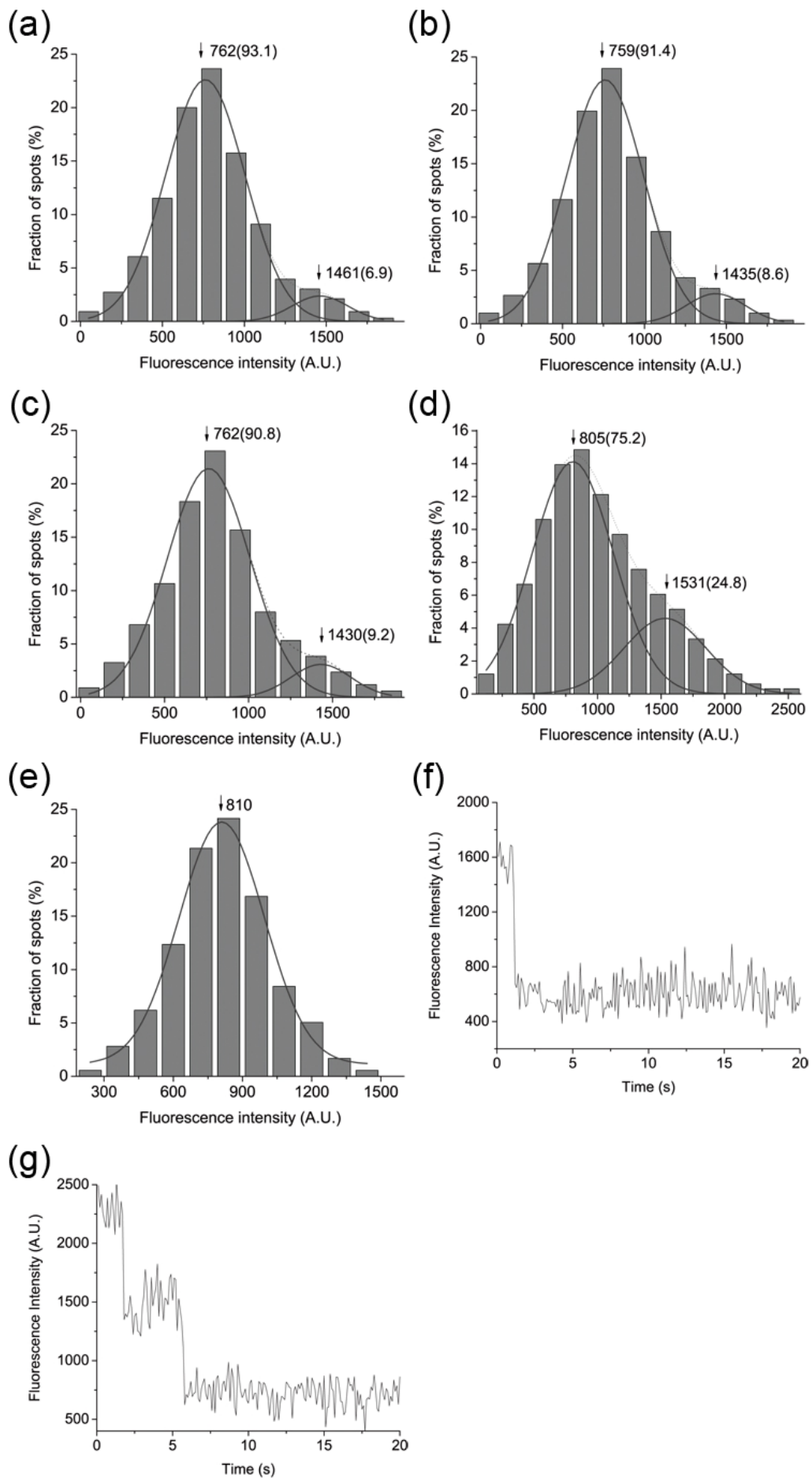


Fig SI-1. Single-molecule fluorescence imaging of T β RII-GFP molecules with the HeLa cells. (a-c) Distributions of the fluorescence intensity of diffraction-limited T β RII-GFP spots from the unstimulated cells without (a) and with 50 μ M (b) or 100 μ M (c) Naringenin treatment. (d) Distribution of the fluorescence intensity of diffraction-limited T β RII-GFP spots from the TGF- β 1-stimulated cells with 50 μ M Naringenin treatment. The solid curves show the fitting of Gaussian function and the two peaks represented T β RII-GFP monomers and dimers, respectively. The arrowheads indicate the peak positions of the fitting curves. Numbers in the parentheses are the fractions. (e) Distribution of the fluorescence intensities of diffraction-limited single GFP molecules ($N = 356$) imaged on coverslips. The solid curve shows the fitting of Gaussian function. The arrowhead indicates the peak position of the fitting curve. (f-g) Two representative time courses of T β RII-GFP emission after background correction show one-step bleaching for a monomer (e) and two-step bleaching for a dimer (f).

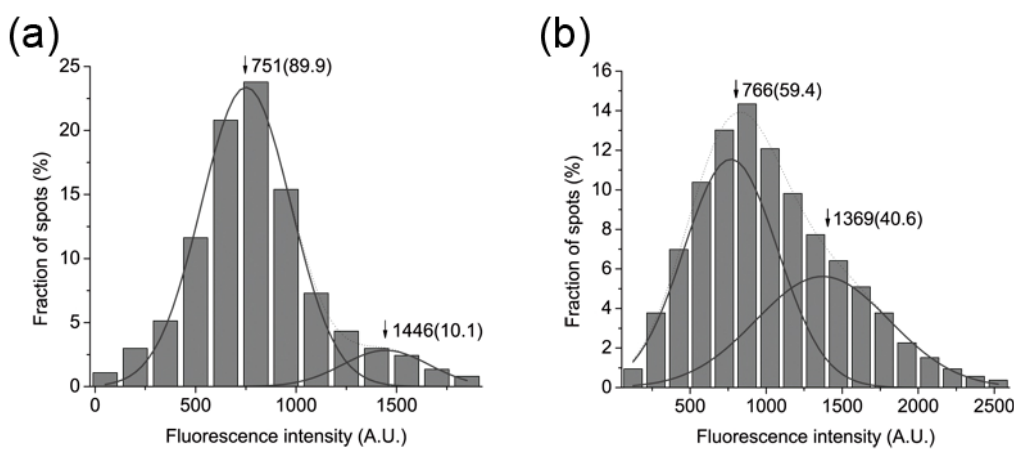


Fig SI-2. Distributions of the fluorescence intensity of diffraction-limited T β RII-GFP

spots from the unstimulated (a) and TGF- β 1-stimulated cells (b) after 100 μ M SB431542 treatment. The solid curves show the fitting of Gaussian function and the two peaks represented T β RII-GFP monomers and dimers, respectively. The arrowheads indicate the peak positions of the fitting curves. Numbers in the parentheses are the fractions.

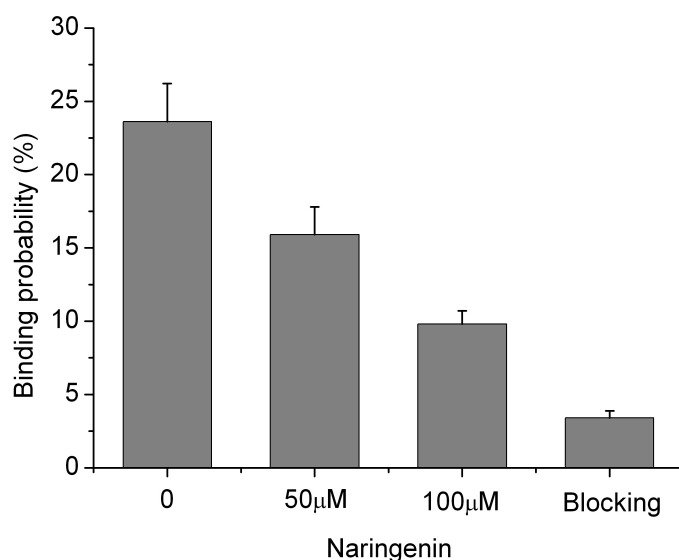


Fig SI-3. The binding probability of TGF- β 1 and T β RII before and after 50 μ M or 100 μ M Naringenin treatment with R1B cells. If the AFM tip was blocked by introducing a solution of T β RII-ECD (5 μ g/mL) to the cell dish, the rupture peak was hardly detected and binding probability reduced dramatically to 3.4% \pm 0.5%. All the experiments were performed repeatedly more than three times.

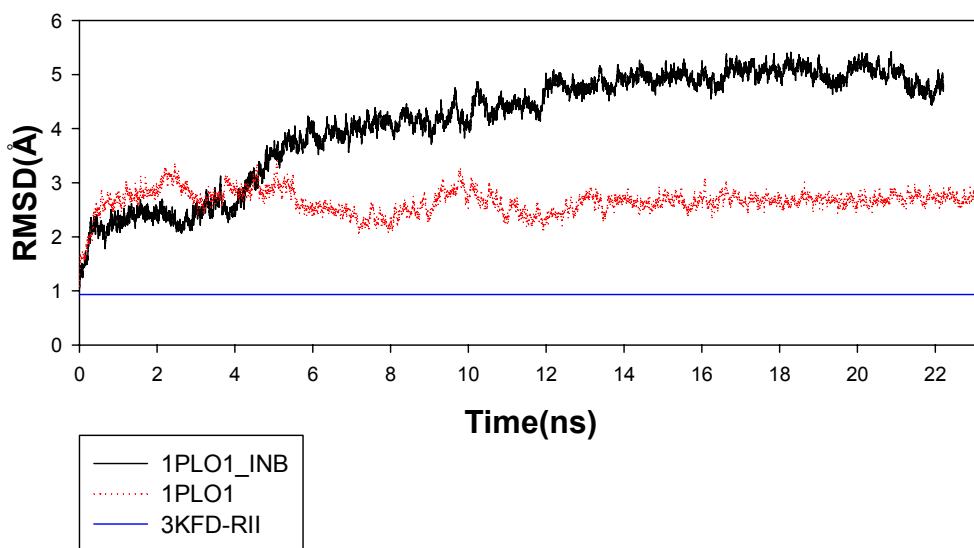


Fig SI-4. Backbone RMSD to first structure. The red curve stands for the T β RII system (1PLO1). The black curve stands for the system of T β RII-Naringenin complex. The blue curve stands for the RMSD of T β RII extracellular domain in the complex of T β RI, T β RII and TGF- β 1 (PDB code 3KFD) to the first NMR structure from 1PLO.

SI Movie 1: Imaging of T β RII-GFP molecules on the cell membrane from the live HeLa cells 4 h after transfection. Duration time: 20s.

References

- 1 W. Zhang, Y. Jiang, Q. Wang, X. Ma, Z. Xiao, W. Zuo, X. Fang, Y. -G. Chen, *Proc. Natl. Acad. Sci. USA.*, 2009, **106**, 15679.
- 2 J. Yu, Q. Wang, X. Shi, X. Ma, H. Yang, Y. -G. Chen, X. Fang, *J. Phys. Chem. B.*, 2007, **111**, 13619.
- 3 G. M. Morris, D. S. Goodsell, R.S. Halliday, R. Huey, W. E. Hart, R. K. Belew and A. J. Olson, *J. Computational. Chemistry.*, 1998, **19**, 1639.
- 4 S. Deep, K. P. 3rd. Walker, Z. Shu, A. P. Hinck, *Biochemistry*, 2003, **42**, 10126.
- 5 S. Joy, P. S. Nair, R. Hariharan, M. R. Pillai, *In. Silico. Biol.*, 2006, **6**, 601.
- 6 D. Wei, H. Zheng, N. Su, M. Deng, L. Lai, *J. Chem. Inf. Model.*, 2010, **50**, 1855.
- 7 (a) D. A. Case, T. E. 3rd. Cheatham, T. Darden, H. Gohlke, R. Luo, K. M. Jr. Merz, A. Onufriev, C. Simmerling, B. Wang, R. J. Woods, *J. Comput. Chem.*, 2005, **26**,

1668. (b) J. W. Ponder, D. A. Case, *Adv. Protein. Chem.*, 2003, **66**, 27.
- 8 L. J. William, C. Jayaraman, D. M. Jeffry, W. I. Roger, L. K. Michael, *Chem. Phys. J.*, 1983, **79**, 926.
- 9 (a) T. Darden, L. Perera, L. Li, L. Pedersen, *Structure*, 1999, **7**, R55. (b) B. A. Luty, M. E. Davis, I. G. Tironi, W. F. Vangunsteren, *Mol. Sim.*, 1994, **14**, 11.
- 10 W. D. Cornell, P. Cieplak, C. I. Bayly, I. R. Gould, K. M. Merz, D. M. Ferguson, D. C. Spellmeyer, T. Fox, J. W. Caldwell, P. A. Kollman, *J. Am. Chem. Soc.*, 1995, **117**, 5179.
- 11 S. E. Feller, Y. H. Zheng, R. W. Pastor, B. R. Brooks, *J. Comp. Phys.*, 1995, **103**, 4613.
- 12 S. Radaev, Z. Zou, T. Huang, E. M. Lafer, A. P. Hinck, P. D. Sun, *J. Biol. Chem.*, 2010, **285**, 14806.